Available online at www.sciencedirect.com
ScienceDirect
Bioorganic & Medicinal Chemistry Letters 18 (2008) 3421–3426
Bioorganic & Medicinal Chemistry Letters

# Novel HCV NS5B polymerase inhibitors derived from 4-(1′,1′-dioxo-1′,4′-dihydro-1′λ$^6$-benzo[1′,2′,4′]thiadiazin-3′-yl)-5-hydroxy-2*H*-pyridazin-3-ones: Part 4. Optimization of DMPK properties

Maria V. Sergeeva, Yuefen Zhou,* Darian M. Bartkowski, Thomas G. Nolan, Daniel A. Norris, Ellen Okamoto, Leo Kirkovsky, Ruhi Kamran, Laurie A. LeBrun, Mei Tsan, Rupal Patel, Amit M. Shah, Matthew Lardy, Alberto Gobbi, Lian-Sheng Li, Jingjing Zhao, Thomas Bertolini, Nebojsa Stankovic, Zhongxiang Sun, Douglas E. Murphy, Stephen E. Webber and Peter S. Dragovich

*Anadys Pharmaceuticals, Inc., Medicinal Chemistry, 3115 Merryfield Row, San Diego, CA 92121, USA*

Received 27 February 2008; revised 30 March 2008; accepted 1 April 2008
Available online 4 April 2008

**Abstract**—5-Hydroxy-3(2*H*)-pyridazinone derivatives were investigated as potent inhibitors of genotype 1 HCV NS5B polymerase focusing on the optimization of their drug metabolism and pharmacokinetics (DMPK) profiles. This investigation led to the discovery of potent inhibitors with improved DMPK properties.


An estimated 3% of the world's population is chronically infected with the hepatitis C virus (HCV), a positive single strand RNA virus of the Flaviviridae family.[1,2] In the United States alone, HCV is estimated to cause 8000–10,000 deaths annually and is now the most common reason for liver transplantation.[3] The current standard of care for the treatment of HCV infection is a combination of pegylated interferon (IFN) with ribavirin.[4] Low response rates, in particular for patients infected with genotype 1 HCV, along with significant side-effects of this therapy result in an urgent medical need for improved HCV treatments.[5]

The discovery of novel, direct antivirals to effectively treat HCV infection therefore remains an area of intense focus for the pharmaceutical industry. The HCV NS5B enzyme, a virally encoded RNA-dependent RNA polymerase (RdRp), is viewed as an attractive target for the development of such direct antiviral agents due to its central role in the replication of the viral genome.[6–8] Accordingly, our research efforts have been focused on developing small molecule, non-nucleoside NS5B inhibitors especially for use in patients infected with HCV genotype 1.

We previously described the discovery and structure-guided optimization of a series of 5-hydroxy-3(2*H*)-pyridazinone-containing NS5B inhibitors that bind to the 'palm' site (**1**, Fig. 1).[9–11] As part of these efforts, compound **1a** (Fig. 1) was identified as one of the most potent molecules in this series with low nanomolar inhibition activity in both enzymatic (genotypes 1a and 1b) and cell-based (1b replicon) assays. Interestingly, compound **1a** accumulated to relatively high levels in rat liver following oral dosing.[11] However, **1a** also exhibited very low bioavailability and low plasma exposures when orally administered to both rats and cynomolgus monkeys.[11] Although we believe that the accumulation of **1a** at a major site of HCV replication could facilitate its use as an anti-HCV agent, we also wished to identify other compounds that afforded more robust plasma exposures following their oral administration. We therefore pursued the further optimization of this series of pyridazinone-containing inhibitors in an effort to improve oral bioavailability.

*Keywords*: Pyridazinones; 5-Hydroxy-3(2*H*)-pyridazinone derivatives; Hepatitis C virus (HCV); RNA-dependent RNA polymerase (RdRp); Small molecule; Non-nucleoside NS5B inhibitors; DMPK properties.
* Corresponding author. Tel.: +1 858 530 3693; fax: +1 858 530 3644; e-mail: yuefen.zhou@gmail.com

0960-894X/$ - see front matter © 2008 Elsevier Ltd. All rights reserved.
doi:10.1016/j.bmcl.2008.04.005

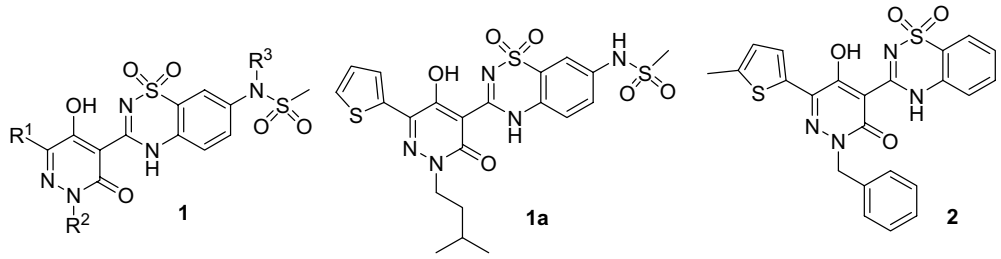


NS5B (1b) $IC_{50}$ = <10 nM
Replicon $EC_{50}$ (1b) = 5 nM
PSA = 203 Å$^2$
$P_{app}$ = 0.02x10$^{-6}$ cm/sec
$P_{app}$ BA/AB ratio = 2375
$F_{po}$ (monkey) = 2% (1 mg/kg)

NS5B (1b) $IC_{50}$ = 4,900 nM
PSA = 148 Å$^2$
$P_{app}$ = 1.3 x10$^{-6}$ cm/sec
$P_{app}$ BA/AB ratio = 6
$F_{po}$ (monkey) = 33% (1 mg/kg)

**Figure 1.** HCV NS5B polymerase inhibitors.

In our previous work, we concluded that the low oral bioavailability exhibited by **1a** was likely due to poor intestinal absorption caused by its highly polar nature and/or its ability to serve as an efficient efflux substrate.[11] To further test this hypothesis, we prepared a metabolically stable control compound (**2**) whose calculated polar surface area (PSA) was much closer to the range typically associated with the well-absorbed molecules (PSA < 140 Å$^2$).[12,13] This compound displayed significantly improved Caco-2 permeability relative to **1a**, a reduced potential for efflux, and dramatically increased oral bioavailability properties in monkeys (Figs. 1, 2, and Table 1). The improvement in oral bioavailability likely resulted from a significant increase in the fraction of **2** that was absorbed following oral administration as compared with **1a** ($FA_{po}$, Table 1).

Encouraged by these results, we focused our pyridazinone optimization strategy on identifying potent NS5B inhibitors with reduced PSA values relative to that of compound **1a**.[14,15] We therefore designed molecules that incorporated $R^1$, $R^2$, and $R^3$ fragments that were (1) less polar than those present in **1a** and (2) known from our previous work to impart potent anti-NS5B properties against both genotypes 1a and 1b polymerases.[9–11] To further differentiate designs with identical PSA values, we also calculated the corresponding fraction absorbed parameter (cFA) using a recently-developed computational algorithm that afforded good correlation with experimental fraction absorbed for a large number of existing drugs (Table 1).[17] Although our previous work suggested that inclusion of the less polar moieties might reduce the metabolic stability of the resulting compounds,[9–11] we believed that the described strategy offered a good opportunity to more optimally balance the overall biological profiles of the inhibitors under study.

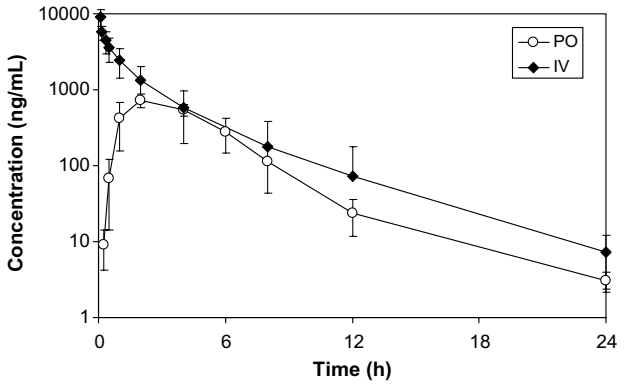


**Figure 2.** Plasma concentrations of compound **2** in monkeys at various times after a single 1 mg/kg dose (administered both IV and PO).

As shown in Table 1, N-methylation of the terminal sulfonamide present in **1a** afforded improvements in Caco-2 permeability, efflux ratio, and in vivo fraction absorbed ($FA_{po}$ = 33%) (compare compound **1b** with **1a**). As anticipated from our earlier work, these improvements were realized at the expense of metabolic stability (in addition to loss of antiviral potency), and this detriment likely attenuated the extent of increase in observed oral bioavailability as compared with **1a** ($F_{po}$ = 12%, relatively low due to high clearance caused by metabolic instability). Interestingly, replacing the isoamyl $R^2$ moiety present in **1b** with a *tert*-butyl ethyl group worsened the corresponding oral bioavailability of the resulting compound **1c**. Consistent with this result, compound **1c** exhibited significantly lower $P_{app}$ and $FA_{po}$ values suggesting that poor absorption was responsible for the observed bioavailability differences. However, since the chemical structures and calculated PSA and cFA values of these two inhibitors are quite similar, we presently do not understand why they exhibit such divergent permeability properties.[21]

Further reduction in the PSA values of the compounds under study was achieved by replacing the $R^1$ thiophene moiety present in **1a**–**c** with alkyl or alkenyl groups (Table 1, **1d**–**n**). Not unexpectedly, the increased lipophilicities of these molecules almost always afforded increased $P_{app}$ values and reduced HLM/MLM stabilities relative to **1a**. One exception was compound **1f** that exhibited $t_{1/2}$ > 60 min in the MLM assay (compare **1f** with **1e**).

**Table 1.** In vitro and in vivo biological properties of pyridazinone NS5B inhibitors

| Compound [a] | $R^1$ | $R^2$ | $R^3$ | PSA (Å$^2$)[b] | cFA[c] (%) | $EC_{50}$ (1b) [d], nM | HLM $t_{1/2}$ (min)[d] | MLM $t_{1/2}$ (min)[e] | $P_{app}$ [f] (cm/s) $\times 10^{-6}$ (AB) | $P_{app}$ BA/AB ratio | $FA_{po}$ [g] (%) | $F_{po}$ [h] (%) |
|---|---|---|---|---|---|---|---|---|---|---|---|---|
| **1a** |  |  | H | 203 | 18 | 5 | >60 | >60 | 0.02 | 2,375 | 4 | 2 |
| **1b** |  |  | $CH_3$ | 194 | 26 | 130 | 28 | 10 | 0.20 | 175 | 33 | 12 |
| **1c** |  |  | $CH_3$ | 194 | 30 | 350 | 26 | 6.7 | 0.01 | ND[i] | 5 | 3 |
| **1d** |  |  | H | 174 | 26 | 320 | 11 | 30 | 0.58 | 10 | 17 | 15 |
| **1e** |  |  | H | 174 | 31 | 54 | 23 | 32 | 0.29 | 62 | 8 | 6 |
| **1f** |  |  | H | 174 | 26 | 69 | 10 | >60 | 0.70 | 24 | 7 | 6 |
| **1g** |  |  | H | 174 | 33 | 62 | 10 | 7 | 0.15 | 100 | 4 | 4 |
| **1h** |  |  | H | 174 | 25 | 370 | 19 | 53 | 0.49 | ND | 9 | 7 |
| **1i** |  |  | H | 174 | 34 | 110 | 7.3 | 10 | 0.85 | 27 | 18 | 15 |
| **1j** |  |  | H | 174 | 36 | 170 | 6.4 | 7.8 | ND | ND | 18 | 10 |
| **1k** |  |  | H | 174 | 22 | 47 | 11 | 6.4 | 0.95 | 15 | 5 | 4 |
| **1l** |  |  | H | 174 | 33 | 30 | 25 | 24 | 0.03 | 433 | 7 | 4 |
| **1m** |  |  | H | 174 | 25 | 22 | 31 | 41 | 0.59 | 36 | 6 | 4 |
| **1n** |  |  | H | 174 | 33 | 16 | 21 | 17 | 1.0 | 17 | 2 | 2 |
| **2** |  |  | NA[j] | 148 | 59 | ND | >60 | >60 | 1.3 | 6 | 36 | 33 |

[a] See Refs. 18 and 19 . The aqueous solubility limit for most compounds was >100 μM except compounds **1k** (>50 μM) and **2** (>80 μM).

[b] Polar surface areas (PSA) were calculated using ACD/Labs, version 10.0, Advanced Chemistry Development, Inc., Toronto ON, Canada, www.acdlabs.com, 2006.

[c] See Ref. 17.

[d] For human liver microsomes (HLM) assay conditions and the experimental error, see Ref. 9. For compounds **1a**–**b**, **1d**, **1h**–**j**, $CC_{50}$ (GAPDH) >33 μM; for compounds **1e**–**g**, **1k**–**n**, $CC_{50}$ > 1 μM (the highest concentration tested); for compound **1d**, $CC_{50}$ > 17 μM (the highest concentration tested).

[e] For monkey liver microsomes (MLM) assay condition and the experimental error, see Ref. 10.

[f] Controls: $P_{app}$ (apparent permeability coefficient) Atenolol (low) = $0.4 \times 10^{-6}$ (cm/s), $P_{app}$ Propranolol (high) = $10 \times 10^{-6}$ (cm/s). AB, apical-to-basolateral; BA, basolateral-to-apical.

[g] $FA_{po}$: Experimental fraction absorbed. It was estimated based on the measured oral bioavailability ($F_{po}$%) and clearance of the compound in animals according to the following formula. $FA_{po} = F_{po}/(1 - CL/Q)$ where $Q$ = 44 mL/min/kg (hepatic blood flow in cynomolgus money).[20]

[h] Dose: 1 mg/kg for all the compounds in cynomolgus monkeys ($n$ = 2–8). Formulation (for both PO and IV administrations): 1% DMSO, 9.9% Cremophor EL in 50 mM sodium phosphate buffer, pH 7.4.

[i] ND = not determined.

[j] NA = compound **2** does not have a 7′-substituent.

**Table 2.** PK parameters for selected compounds dosed in cynomolgus monkeys

| Compound | $n$[a] | $F_{po}$ (%) | $AUC_{inf}$ (ng/h/mL) PO/IV | $C_{max}$ (PO) (ng/mL) | $T_{max}$ (PO) (h) | $C_{12h}$ (PO)/$EC_{50}$ | CL (IV) (mL/min/kg) | $V_{ss}$ (IV) (L/kg) | MLM $t_{1/2}$ (min) | |
|---|---|---|---|---|---|---|---|---|---|---|
| **1a** | 8 × (PO) 8 × (IV) | 2 | 30/1334 | 3.8 | 6.3 | 0.54 | 13.7 | 0.18 | >60 | |
| **1b** | 4 × (PO) 2 × (IV) | 13 | 72/605 | 11 | 6 | 0.032 | 27.8 | 0.57 | 10 | |
| **1d** | 2 × (PO) 4 × (IV) | 15 | 611/3977 | 294 | 1.5 | 0.007 | 4.4 | 0.17 | 30 | |
| **1i** | 2 × (PO) 2 × (IV) | 15 | 370/2541 | 113 | 1.3 | 0.09 | 6.6 | 0.15 | 10 | |
| **1j** | 2 × (PO) 2 × (IV) | 10 | 89/851 | 13 | 6 | 0.02 | 19.6 | 0.57 | 7.8 | |
| **2** | 2 × (PO) 4 × (IV) | 33 | 3654/10897 | 673 | 2 | ND | 1.9 | 0.21 | > 60 | >60 |

[a] $n$, number of monkeys used in the PK study. Dose: 1 mg/kg. Formulation (for both PO and IV administration): 1% DMSO, 9.9% Cremophor EL in 50 mM sodium phosphate buffer, pH 7.4.

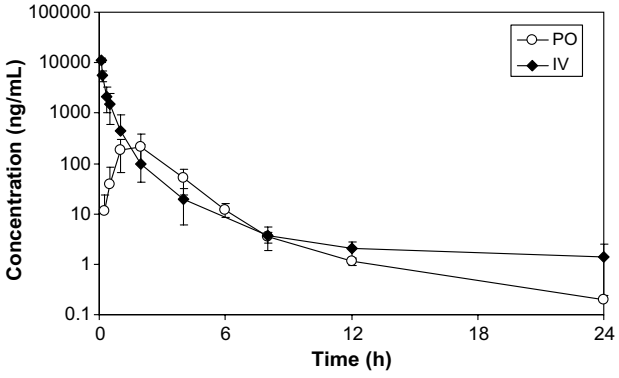


**Figure 3.** Plasma concentrations of compound **1d** in monkeys at various times after a single 1 mg/kg dose (administered both IV and PO) in cynomolgus monkeys.

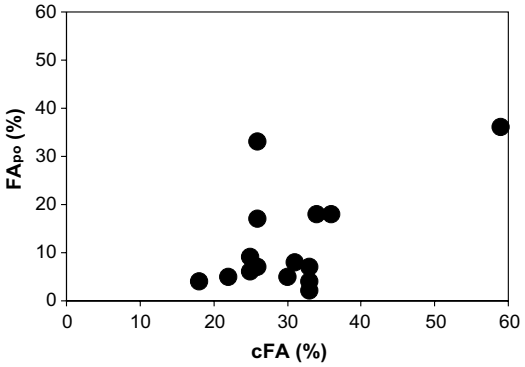


**Figure 5.** Plot of calculated fraction absorbed (cFA) versus in vivo $FA_{po}$ (%).

Unfortunately, the majority of these compounds also exhibited minimal improvements relative to **1a** in both in vivo fraction absorbed ($FA_{po}$) and bioavailability properties ($F_{po}$) following oral administration to monkeys. Notable exceptions included inhibitors **1d**, **1i**, and **1j** each of which displayed improved in vivo bioavailability and in vivo $FA_{po}$ values as compared with the lead molecule (**1a**). In addition to lower PSA properties, all these compounds had significantly higher cFA and $P_{app}$ values as compared with **1a**. While we believe that these differences likely contributed to their improved oral bioavailabilities, related improvements in bioavailability were not observed for compounds **1k** and **1n** which also possessed similarly favorable PSA, cFA and even higher $P_{app}$ values.

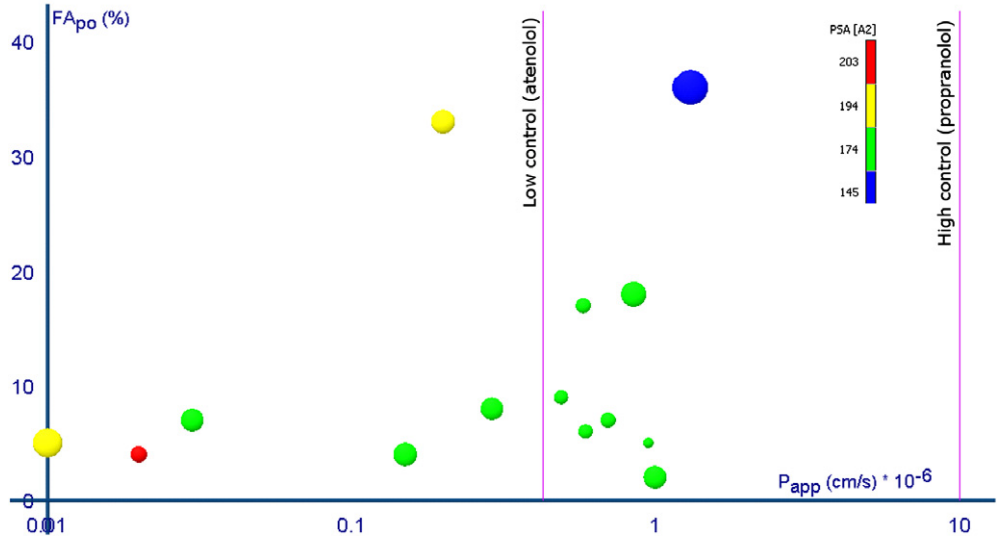


**Figure 4.** Correlations between in vitro $P_{app}$, in vivo $FA_{po}$, calculated PSA, and calculated log $D$ values for the compounds listed in Table 1. The size of the solid circles represents the value of the log $D$ at pH 6.0 calculated using ACD/Labs software, version 10.0, Advanced Chemistry Development, Inc., Toronto ON, Canada, www.acdlabs.com, 2006. For the smallest solid circle, log $D$ = − 2.25 (pH 6), and for the largest solid circle, log $D$ = 0.29 (pH 6). The low ($0.4 \times 10^{-6}$ cm/s) and high ($10 \times 10^{-6}$ cm/s) $P_{app}$ values for the controls are marked with purple lines. Compound **1j** was not included in this Figure as its $P_{app}$ value was not determined. This figure was generated using the Miner3D software.

Table 2 details the PK parameters for selected inhibitors (**1b**, **1d**, **1i**–**j**) that exhibited $F_{po} \geqslant 10\%$ when dosed in cynomolgus monkeys at 1 mg/kg. The IV and oral PK curves associated with inhibitor **1d** are also shown in Figure 3. All these compounds exhibited low to moderate clearance and low steady-state volumes of distribution (<1 L/kg) with moderate to good antiviral potency (1b $EC_{50}$ = 110–320 nM). Although these molecules showed an improvement in both oral bioavailability and $C_{max}$ parameters as compared with **1a**, they exhibited significantly lower $C_{12h}/EC_{50}$ ratios. In addition, MLM stability for these compounds did not correlate well with the corresponding clearance data suggesting that this process may not be primarily mediated via biotransformation. Collectively, these results illustrate the challenges we faced in optimizing the DMPK properties of the molecules in this series.

In order to further improve the oral bioavailability and retain the antiviral potency of this series of pyridazinone compounds, we performed several analyses (Figs. 4 and 5 ) to help identify which calculated parameter, measured property, or combination thereof conferred the beneficial in vivo performance to the molecules shown in Table 1.

As shown in Figure 4, molecules that possessed lower PSA values had a greater chance of exhibiting Caco-2 permeabilities in excess of the low control ($0.4 \times 10^{-6}$ cm/s). The more permeable compounds ($P_{app}$ > low control), in turn, had an increased likelihood of displaying in vivo $FA_{po}$ values above 10%. Collectively, this analysis confirmed that reduction in PSA values could favorably impact the permeability properties of the pyridazinone-containing NS5B inhibitors described in this work. However, for compounds with identical PSA characteristics (e.g., 174 $Å^2$), the in vivo fraction absorbed ($FA_{po}$) varied from 2% to 18%. In addition, there was little correlation noted between logD values and the in vivo fraction absorbed. Consistent with this observation, the calculated fraction absorbed (cFA) values (which were based on both calculated PSA and calculated logD) associated with the above compounds showed little to no correlation with the corresponding experimental fraction absorbed parameters (Fig. 5).[22] Caveats associated with the described analyses of Figures 4 and 5 include (1) the relatively small number of data points examined and (2) the lack of compounds with moderate to high permeability properties (needed to better define trends over a wide range of $P_{app}$ and cFA values).

In summary, a number of potent inhibitors of genotype 1 HCV NS5B polymerase derived from pyridazinones were evaluated in both in vitro assays and in vivo animal PK studies. The described optimization focused on DMPK properties and led to potent inhibitors (1b $EC_{50}$ = 110–320 nM) with improved oral bioavailabilities (10–15%) relative to the lead compound (**1a**, 2%). In addition, analysis of the correlation between calculated parameters, in vitro biological properties, and the measured fraction absorbed or oral bioavailability in animals defined relationships that could be applied in the further optimization of the DMPK properties of the molecules in this series.

## Acknowledgments

The authors thank Drs. Devron Averett and Steve Worland for their support and helpful discussions during the course of this work. The authors also thank Dr. James Appleman for helpful discussions during the preparation of this manuscript.

## References and notes

1. WHO, Hepatitis C fact Sheet No. 164. Revised October 2000. http://www.who.int/mediacentre/factsheets/fs164/en, (2000).
2. Lauer, G. M.; Walker, B. D. *N. Engl. J. Med.* **2001**, *345*, 41.
3. McHutchison, J. G. *Am. J. Manag. Care* **2004**, *10*, S21.
4. (a) Sidwell, R. W.; Huffman, J. H.; Khare, G. P.; Allen, L. B.; Witkowski, J. T.; Robins, R. K. *Science* **1972**, *177*, 705; (b) Smith, R. A.; Kirkpatrick, W.. In *Ribavirin, a Broad Spectrum Antiviral Agent*; Academic Press: New York, 1980; Vol. xiii, p 237; (c) De Clercq, E. *Adv. Virus Res.* **1993**, *42*, 1.
5. Hoofnagle, J. H.; Seeff, L. B. *N. Eng. J. Med.* **2007**, *355*, 2444.
6. Appel, N.; Schaller, T.; Penin, F.; Bartenschlager, R. *J. Biol. Chem.* **2006**, *281*, 9833.
7. Koch, U.; Narjes, F. *Infect. Disorders: Drug Targets* **2006**, *6*, 31.
8. Condon, S. M.; LaPorte, M. G.; Herbertz, T. *Curr. Med. Chem. Anti-Infective Agents* **2005**, *4*, 99.
9. Zhou, Y.; Webber, S. E.; Murphy, D. E.; Li, L.-S.; Dragovich, P. S.; Tran, C. V.; Sun, Z.; Ruebsam, F.; Shah, A. M.; Tsan, M.; Showalter, R. E.; Patel, R.; Li, B.; Zhao, Q.; Han, Q.; Hermann, T.; Kissinger, C. R.; LeBrun, L.; Sergeeva, M. V.; Kirkovsky, L. *Bioorg. Med. Chem. Lett.* **2008**, *18*, 1413.
10. Zhou, Y.; Li, L.-S.; Dragovich, P. S.; Murphy, D. E.; Tran, C. V.; Ruebsam, F.; Webber, S. E.; Shah, A. M.; Tsan, M.; Averill, A.; Showalter, R. E.; Patel, R.; Han, Q.; Zhao, Q.; Hermann, T.; Kissinger, C. R.; LeBrun, L.; Sergeeva, M. V. *Bioorg. Med. Chem. Lett.* **2008**, *18*, 1419.
11. Li, L.-S.; Zhou, Y.; Murphy, D. E.; Stankovic, N.; Zhao, J.; Dragovich, P. S.; Bertolini, T.; Sun, Z.; Ayida, B.; Tran, C. V.; Ruebsam, F.; Webber, S. E.; Shah, A. M.; Tsan, M.; Showalter, R. E.; Patel, R.; LeBrun, L. A.; Bartkowski, D. M.; Nolan, T. G.; Norris, D. A.; Kamran, R.; Brooks, J.; Sergeeva, M. V.; Kirkovsky, L.; Zhao, Q.; Kissinger, C. R. *Bioorg. Med. Chem. Lett.* **2008**, *18*, 3446.
12. (a) Veber, D. F.; Johnson, S. R.; Cheng, H.-Y.; Smith, B. R.; Ward, K. W.; Kopple, K. D. *J. Med. Chem.* **2002**, *45*, 2615; (b) Palm, K.; Stenberg, P.; Luthman, K.; Artursson, P. *Pharm. Res.* **1997**, *14*, 568.
13. We chose to include methylated thiophene as $R^1$ and benzyl as $R^2$ groups in control compound **2** since these entities were known to increase metabolic stability (at the expense of anti-NS5B potency).
14. The weak NS5B inhibition activity exhibited by compound **2** prevented its further development as an anti-HCV agent.
15. An alternate optimization strategy of reducing the affinity of the pyridazinones for intestinal efflux pumps was not

pursued at this time. As many efflux pump substrates are often highly lipophilic in nature,[16] exploration of this strategy would likely involve compound modifications that increased (rather than reduced) PSA values.

16. (a) Stoch, T. R.; Gudmundsson, O. *Adv. Drug. Del. Rev.* **2002**, *54*, 315; (b) Cianchetta, G.; Singleton, R. W.; Zhang, M.; Wildgoose, M.; Giesing, D.; Fravolini, A.; Cruciani, G.; Vaz, R. J. *J. Med. Chem.* **2005**, *48*, 2927.
17. Linnankoski, J., Makela, J. M., Ranta, V.-P., Urtti, A., Yliperttula, M. *J. Med. Chem.* **2006**, *49*, 3674. Calculated fraction absorbed (cFA) values were obtained according to the formula: $cFA = 1 - [1 + 10^{(0.623-0.154\times \log D - 0.007 \times PSA)}]^{-7}$ where log*D* (pH 6.0) and PSA values were calculated using ACD/Labs version 10.0 software (Advanced Chemistry Development, Inc., Toronto ON, Canada, www.acdlabs.com, 2006).
18. All structures of compounds under study were consistent with $^{1}H$ NMR and LC-MS analysis ($\geqslant$95% HPLC purity). They are arbitrarily drawn in one of the possible tautomer forms. The synthesis of these compounds was very similar to that described in Ref. 11.
19. The aqueous solubility limit was determined by UV absorption using the NS5B 1b enzymatic assay conditions (2% DMSO in 20 mM Tris–HCl, pH 7.5, 20 mM NaCl, 5 mM $MgCl_2$, 5 mM dithiothreitol, 0.1 g/L).
20. Davies, B.; Morris, T. *Pharm. Res.* **1993**, *10*, 1093.
21. We cannot exclude the possibility that compound **1c** is a more efficient efflux substrate than **1b**.
22. One explanation for this lack of correlation is the high PSA values of the pyridazinones described in this work (all $\geqslant$140 Å$^2$) relative to the majority of compounds used to derive the formula listed in reference 17 (most <130 Å$^2$).